Research Square

Preprints are preliminary reports that have not undergone peer review.
They should not be considered conclusive, used to inform clinical practice,
or referenced by the media as validated information.

Class-switched CD21 + CD27 + memory B cells as a predictive immunological marker of vaccine-induced humoral responsiveness in Common Variable Immunodeficiency

Laura Fernandez Blanco

l.fernandezblanco@sanquin.nl

Sanquin Research and Landsteiner Laboratory of the Academic Medical Center

Rebeca Gutiérrez-Cózar

Sanquin Research and Landsteiner Laboratory of the Academic Medical Center

Tineke Jorritsma

Sanquin Research and Landsteiner Laboratory of the Academic Medical Center

Liubov Babii

Sanquin Research and Landsteiner Laboratory of the Academic Medical Center

Rebecca Cornelis

Sanquin Research and Landsteiner Laboratory of the Academic Medical Center

Juan J. Garcia Vallejo

Amsterdam UMC Location Vrije Universiteit Amsterdam

Marit J. van Gils

Amsterdam UMC Location University of Amsterdam

Filip Eftimov

Amsterdam UMC Location University of Amsterdam

Jelle de Wit

Centre for Infectious Disease Control, National Institute for Public Health and the Environment

Virgil A.S.H. Dalm

Erasmus MC

Rory D. de Vries

Erasmus MC

Debbie van Baarle

University Medical Center Groningen

Anja ten Brinke

Sanquin Research and Landsteiner Laboratory of the Academic Medical Center

S. Marieke van ham

Sanquin Research and Landsteiner Laboratory of the Academic Medical Center

Research Article

Keywords: Common Variable Immunodeficiency, predictive biomarkers, B-lymphocytes, antibody formation, COVID-19 vaccination, CD21+ memory B cells, humoral response

Posted Date: November 10th, 2026

DOI: https://doi.org/10.21203/rs.3.rs-11458239/v1

License: This work is licensed under a Creative Commons Attribution 4.0 International License.
Read Full License

Additional Declarations: Competing interest reported. FE reports grants from ZonMw for COVID-19 research (#10430072010007). VASHD received consulting fees from GlaxoSmithKline, Pharming NV for Advisory board meetings and honoraria for lectures from Takeda Pharmaceutical Company, Kedrion, AstraZeneca.

Abstract

Common variable immunodeficiency (CVID) is a clinically heterogeneous primary immunodeficiency characterized by defective humoral immunity and highly variable vaccine-induced antibody responses. However, in-depth characterization of vaccine-specific B cell responses in CVID remains limited, hindering our understanding of the cellular basis of this heterogeneity.

Here, we investigated how CVID affects formation and maintenance of antigen-specific B cell responses following COVID-19 mRNA-based vaccination of patients who either do (responders; R) or do not (non-responders; NR) seroconvert. The evolution of the spike (S)-specific B cell compartment was longitudinally investigated after vaccination and compared to RSV-F-specific B cells, as a historically encountered antigen, and the total B cell compartment.

CVID-NR patients showed pronouncedly reduced S-specific B cell numbers at all time points compared to CVID-R and healthy donors. Additionally, the S-specific B cell compartment showed a predominantly naïve, unswitched phenotype. CVID-R exhibited a delayed S-specific B cell differentiation, with a markedly naïve, unswitched response after the first vaccination, an enhanced response after the second vaccination with reduced IgG^+ memory B cells, and a fully established S-specific B cell compartment 6 months after vaccination. Analysis of the general B cell compartment showed strongly diminished class-switched B cell populations in NR patients, emerging as a predictive immunological marker for vaccine-induced humoral responsiveness in CVID.

Together, these findings reveal distinct cellular alterations underlying vaccine responsiveness in patients with CVID and identify potential correlates of humoral vaccine responses, stablishing a framework for more personalized immune monitoring strategies in CVID.

Introduction

Common variable immunodeficiency (CVID) is the most common symptomatic primary immunodeficiency, characterized by marked clinical and biological heterogeneity. It is defined by reduced serum IgG and IgA, with or without reduced IgM, and absent or impaired responses to polysaccharide vaccination [1, 2]. Clinical findings include recurrent upper and lower respiratory tract infections and gastrointestinal tract infections. Additionally, many patients develop non-infectious complications, including autoimmunity and/or autoinflammation, lymphoproliferation, and granulomatous disease [3, 4]. Although CVID is classically described as a humoral defect, multiple other immune cell populations, including T cells and myeloid cells, may also be affected [5–9].

Given the crucial role of antibodies in protection against viral infections, patients with CVID are particularly susceptible to severe viral disease and frequently exhibit impaired responses to vaccination. During the COVID-19 pandemic, multiple observational studies reported increased rates of severe disease and mortality in patients with CVID compared with healthy individuals [10–14]. Consistent with these clinical observations, studies on influenza vaccination have shown reduced circulating

hemagglutinin-specific memory B cells (MBCs) in patients with CVID, suggesting impaired vaccine-induce immunity in this population [15–17]. Building on these observations, we and others investigated immune responses to COVID-19 vaccination and found reduced immunogenicity in patients with CVID, including diminished binding and neutralizing antibody titers and weaker T cell responses [18–21]. In the longitudinal study by van Leeuwen LPM *et. al*, a substantial proportion of CVID patients failed to mount detectable antibodies after two vaccine doses, and those who did often showed a faster decline in antibody levels compared to healthy individuals [21] Notably, the study cohort was predominantly composed of CVID patients with non-infectious complications, including autoimmune manifestations, many of whom were receiving immunosuppressive therapy. Together, these findings highlight the vulnerability of CVID patients to viral infections and underscore the need to better understand the mechanisms underlying protective vaccine-induced immunity. In particular, it remains unknown why only a subset of patients with CVID develops detectable antibody responses after vaccination and why the kinetics and durability of these responses differ from those of healthy individuals.

Circulating antibodies produced by antibody-secreting cells (ASCs), play a key role in immune protection. Longitudinal studies, including those by us, have comprehensively characterized the phenotype and dynamics of S-specific B cells following COVID-19 vaccination [22–26]. Following antigen exposure, an early extrafollicular (EF) pathway leads to the formation of short-lived ASCs and early MBCs [27]. Additionally, germinal centers (GCs) are formed in secondary lymphoid organs leading to the generation of high-affinity ASCs and long-lived MBCs [28–31]. Several studies have investigated Activated B cells (ActBCs), defined as $CD27^+$ $CD21^{low}$ $CD71^+$, which represent a transient population that has recently exited the GC and may precede MBC and ASC formation [22, 23, 26, 32, 33]. A substantial proportion of ActBCs expresses CD11c, traditionally associated with EF responses, suggesting a broader functional role for CD11c during active immune responses (22). Furthermore, the MBC compartment has been demonstrated to be heterogeneous, extending beyond the classical $CD27^+$ IgD^- definition [22, 23, 34]. Expression of CD73 distinguishes longer-lived MBCs from more recently generated ones. EF-associated responses have classically been linked to DN2 ($CD27^-$ $CD21^-$ $CD11c^+$) and IgD/IgM^+ $CD21^-$ $CD11c^+$ ActBCs [35, 36] but recent findings highlight DN1 ($CD27^-$ $CD21^+$) as an EF-derived long-lived MBC subset and DN3 ($CD27^-$ $CD21^-$ $CD11c^-$) as a potential ASC precursor [37–39].

Various abnormalities affecting B cell differentiation have been reported in CVID. Several studies of the B cell compartment have reported defects in pre-GC B cells, reduced frequencies of MBCs and ASCs, persistent activation of naïve B cells, and expansion of $CD21^-$/low B cells, collectively indicating disruptions in both GC and EF pathways [40–43]. However, how these defects affect vaccine-induced responses remains poorly understood, highlighting the need to characterize antigen-specific B cell differentiation at high-resolution to better understand immune dysfunction in CVID.

In this study, we performed a longitudinal, in-depth characterization of SARS-CoV-2 S-, respiratory syncytial virus fusion glycoprotein (RSV-F)-specific B cells, and total B cells after COVID-19 vaccination to elucidate cellular features underlying impaired vaccine responses in CVID patients. We aimed to

clarify the mechanisms driving heterogeneous vaccine responsiveness by integrating cellular readouts with antibody measurements and comparing responders (R) with non-responders (NR).

Our data show that CVID-NR have markedly reduced S-specific B cells with a predominantly naïve, unswitched phenotype throughout all time points, whereas CVID-R mount a delayed yet eventually comparable response to healthy donors only 6 months after vaccination. Next to these, we observed disruptions in the RSV-F-specific compartment, particularly in GC differentiation and long-lived MBC formation. Overall, our data provide an integrated view of B cell dysregulation in CVID and clarify cellular characteristics underlying heterogeneity in vaccine responsiveness.

Methods

Sex as a biological variable

Our human study examined both male and female subjects and sex distribution was matched between our study groups.

Study design and patient inclusion

This study is a sub-study of the HARMONY research study, combining prospective studies on the efficacy of COVID-19 vaccination in individuals at higher risk of severe SARS-CoV-2 infection. Samples were obtained from seven university hospitals from the Netherlands. In total 68 donors were used for the measurement of antigen-specific B cells, including 12 patients with CVID, 8 with Down Syndrome (DS), 14 with solid tumors (ST), 10 with Multiple Myeloma (MM), 14 HIV and 10 healthy donors (HD). All further analyses were performed only with the 12 CVID patients. Seroconversion was assessed based on anti-S IgG titers, stratifying patients into responders (CVID-R) and non-responders (CVID-NR) (**Figure S1A)**. Exclusion criteria were previous SARS-CoV-2 infection or occurrence of SARS-CoV-2 infection during the study period (as evidenced by positive anti-receptor binding domain (RBD) antibodies before first vaccination and/or self-reported positive PCR or positive anti-nucleocapsid protein antibodies before or throughout the study period). All study participants received two mRNA-based COVID-19 vaccinations with an interval of 28 days according to the Dutch COVID-19 vaccination program. Participants were vaccinated between March and April 2021 with the mRNA-1273 (Moderna) vaccine. Peripheral blood mononuclear cells (PBMCs) were cryopreserved until further use.

Probe design

Recombinant soluble proteins, including SARS-CoV-2 S-2P, RBD and RSV prefusion stabilized F (DS-Cav1) were produced as described before [23, 44]. After purification, proteins were biotinylated with a BirA500 biotin-ligase reaction kit (Avidity) according to manufacturer’s protocol.

B cell spectral flow cytometry staining

PBMCs were thawed in IMDM (Lonza) with 10% FCS (Bodinco BV). Platelets were removed by spinning down at 120 g without brake. Erythrocytes were removed from suspension using RBC Lysis Buffer (in-house) for 10 minutes at room temperature. Approximately 10 x 10^6 PBMCs were enriched for B cells using CD3 T cell and CD14 cell depletion by combining the EasySep™ Human CD3 Positive Selection Kit II and the EasySep™ Human CD14 Positive Selection Kit II (StemCell Technologies) according to manufacturer's instruction. To stain antigen-specific B cells, biotinylated protein antigens SARS-CoV-2 S, RBD and RSV-F were individually multimerized with fluorochrome-conjugated streptavidin in a 2:1 molar ratio at 4°C for 1 hour. Next, 10% D-biotin (GeneCopoeia) was added and incubated at 4°C for at least 30 minutes to block free sites on the streptavidin and reduce cross-reactivity among biotinylated protein antigens. Both biotinylated antigens were conjugated to two fluorochromes, except RBD, which was conjugated with a single fluorochrome and gated as part of S1 (**Table S1**). A 31-color spectral cytometry panel, including the antigen probes, was designed to phenotype antigen-specific B cells (**Table S2**). Enriched B cell samples were first stained using Live/Dead Fixable Blue Stain Kit (Invitrogen) in PBS at 4°C for 30 min. Subsequently, cells were washed twice with staining buffer (PBS supplemented with 1% BSA and 1mM EDTA) and stained with anti-IgG for 10 min at 4°C and immediately after with the specific antibody mix and antigen multimer cocktail for 30 min at 4°C. Next, cells were washed twice with PBS, fixed with 1% paraformaldehyde for 10 minutes at 4°C and washed twice again with staining buffer. Data were acquired on Cytek Aurora 5L spectral cytometer using SpectroFlo® software (Cytek Biosciences).

Spectral flow cytometry data pre-processing

After spectral unmixing (SpectroFlo v3.0.1, Cytek), FCS files were loaded into OMIQ analysis software (www.omiq.ai). Data were transformed using arcsinh with cofactors adequate for each parameter to display a Gaussian distribution of negative populations while maximizing the range of positive values. Initial gating was performed to select single, live cells. PeacoQC was then run on live cells to detect and remove flow cytometry anomalies in both signal acquisition and dynamic range [45]. $CD19^+$ $DUMP^-$ (CD3, CD4, CD16, CD56) cells were then gated. To exclude batch effects, all data were normalized using Cytonorm for 8 markers (CD20, CD24, CD73, CD45RB, HLA-DR, CXCR4, IgD, IgM) based on a reference sample consisting of PBMCs from a single healthy donor included and measured in every batch [46]. Subsequently, for the antigen-specific analysis negative gates were set for each combination of probes, after which antigen-specific B cells were further positively gated based on their specific combinations of fluorochrome-conjugated streptavidin (**Figure S1B, C**). For downstream analysis, data were subsampled to include only all detected antigen-specific B cells (n = 55,000). For the general B cell compartment analysis, 50,000 $CD19^+$ non-S-specific B cells were subsampled per file when possible.

Dimensionality reduction and FlowSOM clustering

For UMAP visualization and FlowSOM clustering (xdim 16, ydim 16), input consisted of a selection of 14 markers (CD20, CD21, CD27, CD24, CD38, CD71, CD73, CD138, CD11c, CD45RB, IgA, IgD, IgM, IgG). For the antigen-specific B cell analysis, data from 68 participants of the HARMONY study cohort were used to obtain maximal resolution. K = 55 FlowSOM clusters were manually merged and annotated into 27 clusters and 17 main B cell populations based on UMAP visualization, heatmap analysis of median marker expression between clusters, and manual gating of specific marker combinations (**Table S3**). Further downstream analysis was performed using only data from the 12 CVID participants and 8 HD included in the current study. For the general B cell compartment analysis, UMAP visualization and FlowSOM clustering was performed as described above only using CVID and HD files as input. K = 30 FlowSOM clusters were manually merged and annotated into 12 main populations (**Table S4**). For the switched and ASC compartment analysis, all IgG^+ and IgA^+ (gated from IgD^- IgM^-) and ASCs were combined. K = 30 FlowSOM clusters were manually merged and annotated into 11 main populations (**Table S5**). Percentages of main B cell populations within the switched compartment analysis are calculated and depicted as percentage within $CD19^+$ live B cells using the total proportion of IgG^+, IgA^+, and ASCs within the $CD19^+$ B cell compartment, determined by manual gating. This analytical workflow followed previously established methods from our group and collaborators [22, 23].

ELISA and neutralization assays

Assays measuring antibody levels were described previously [47]. In summary, S-specific IgG and RBD-specific IgG were measured by a quantitative Luminex assay and expressed as international binding antibody units per mL (BAU/ml). Participants with S-specific IgG above 44.8 BAU/ml were considered seropositive. Of note, intravenous immunoglobulin (IVIG) replacement therapy did not interfere with the antibody measurements, as the preparations used did not contain S-specific antibodies (47). To measure neutralizing antibody levels, a plaque reduction neutralization test (PRNT) using ancestral SARS-CoV-2 was performed as described previously [48].

Study approval

This work was conducted as part of the national HARMONY-COP project (#10430072010005), which provides a unified framework for coordinated COVID-19 vaccine studies and overarching analyses across participating Dutch research groups. The present sub-study analyses samples from the Vaccination Against COvid in Primary Immune Deficiencies (VACOPID) cohort, a prospective, controlled, multicenter study performed in seven university hospitals in the Netherlands. VACOPID was conducted in accordance with the Declaration of Helsinki and approved by the Dutch Central Committee on Research Involving Human Subjects (CCMO, NL7647.078.21, EudraCT 2021–000515-24), the Erasmus MC Medical Research Ethics Committee (MEC-2021–0050), and local institutional review boards. Written informed consent was obtained from all participants prior to enrolment.

Data availability

All data needed to evaluate the conclusions in the paper are present in the paper and/or the Supplementary Materials.

Statistical analysis

Statistical analysis, graphs, heatmaps, volcano plots and stacked bar graphs were made using Rstudio (version 4.1.1) and GraphPad Prism 9.1.1 (GraphPad Software, Boston, MA). Computational analysis of data to generate heatmaps was performed using the Spectre R package. Statistical significance was assessed using t-test or, for non-parametric data, Mann-Whitney test when comparing two groups, and one-way ANOVA or, for non-parametric data, the Kruskal-Wallis test when comparing three groups. Tukey's correction or, for non-parametric data, Dunn's correction was used to correct for multiple testing. Receiver operating characteristic (ROC) analysis was performed to determine the optimal cut-off value for group discrimination. For volcano plots, p-values were corrected for multiple comparison using the Benjamini and Hochberg method. P-values of < 0.05 were considered significant.

Results

Differential S-specific B cell responses in CVID patients

To characterize alterations in the B cell compartment associated with the impaired humoral response to COVID-19 vaccination in CVID, 12 CVID patients and 8 age- and sex-matched HD were selected from the previously described vaccination cohort (Fig. 1A, Table 1**)** [21]. Peripheral blood was collected before vaccination (V1pre), 28 days after first vaccination (V1D28), 28 days after second vaccination (V2D28) and 6 months post-second vaccination (V2M6). CVID-R showed similar antibody kinetics to HD across post-vaccination timepoints, with modestly lower antibody levels, whereas CVID-NR failed to seroconvert and displayed markedly reduced titers at all measured timepoints (**Figure S1A**) [21]. Frequencies and dynamics of the S-specific B cell response following SARS-CoV-2 vaccination were examined first (Fig. 1B, **Figure S1B, C**). The CVID-R group showed a trend toward lower frequencies of S-specific B cells 28 days after the first vaccination, that was not found 6 months after (Fig. 1B, **Figure S1D**). Similar dynamics were observed for RBD-specific B cells (Fig. 1C, **Figure S1D**). When only comparing between CVID groups, CVID-NR displayed lower S- and RBD-specific B cell frequencies than CVID-R at V2D28 (**Figure S1E**). Due to low number of samples and cell counts for CVID-NR at V2M6, this timepoint was excluded for further analyses.

To dissect the evolution of the antigen-specific B cell response, UMAP dimensionality reduction followed by FlowSOM clustering was applied to all S- and RSV-F-specific $CD19^+$ B cells. This clustering approach identified 27 clusters, which were grouped into 17 main B cell populations capturing both GC and EF differentiation pathways (Fig. 1D, **Figure S1F, Table S3**). Within the IgG^+ compartment, two main MBCs populations were identified, with the resting MBCs expressing CD73, and four ActBCs clusters were

defined by variation in CD27, CD45RB and CD11c expression. Also, EF clusters DN1 (IgD^- $CD27^-$ $CD21^+$ $CD11c^-$), DN2 (IgD^- $CD27^-$ $CD21^-$ $CD11c^+$) and DN3 (IgD^- $CD27^-$ $CD21^-$ $CD11c^-$) were identified. MBCs, ActBCs and DN2 populations were also observed for IgA^+ B cells (22,23). Of note, although ASCs could be detected, this compartment may be underestimated due to their sensitivity to freeze–thawing, the early sampling time point (day 7 versus the more commonly used day 28), and the absence of surface B cell receptor (BCR), which precludes their identification as antigen-specific cells [22, 49, 50]. In line with time elapsed since antigen exposure, S- and RSV-F-specific B cells showed distinct distributions across the UMAP, with S-specific cells being mainly present in IgG^+ activated and recently established memory compartments, and RSV-F-specific cells localized within naïve IgD/IgM^+ and resting IgG^+ and IgA^+ MBC populations (Fig. 1D).

Assessing the longitudinal dynamics of the evolution of the S-specific B cell compartment in CVID versus HD, we observed no evidence of IgG^+ and IgA^+ differentiation in CVID-NR across timepoints, with only naïve, unswitched clusters detected, in particular, anergic naïve B cells, defined as IgD^+ IgM^{low} $CD73^+$ B cells **(**Fig. 2A). On the other hand, a delay in differentiation was observed in CVID-R with class-switched populations becoming detectable only after the second vaccine dose (Fig. 2A-D, **Figure S2A**). At V1D28, the S-specific B cell compartment was predominantly composed of naïve and unswitched populations, with anergic naïve B cells representing the dominant population in CVID-R. Several IgG^+ and IgA^+ subsets were reduced compared with HD, with differences in IgG^+ ActBCs, DN3, and IgA^+ MBCs remaining significant after correction for multiple testing (Fig. 2A, B, D). At V2D28, uncorrected analyses indicated lower frequencies of IgG^+ resting MBCs, IgG^+ MBCs and IgA^+ ActBCs in CVID-R; although not significant after correction for multiple testing (Fig. 2C, D). By V2M6, no differences between CVID-R and HD were detected (**Figure S2A**). However, DN3 showed a higher fold change in CVID-R compared to HD (**Figure S2A, B**).

Given that both antibody quality and quantity are important for humoral protection, we evaluated the neutralizing capacity of serum IgG across timepoints. CVID-NR did not have detectable neutralization capacity at any time point. Despite exhibiting total anti-S IgG titers similar to those of HD at V1D28, CVID-R exhibited reduced neutralization capacity at this timepoint (Fig. 2E). At V2D28 and V2M6 however, neutralization in CVID-R was comparable to HD. These results mirror the cellular findings, indicating that although CVID-R generate anti-S IgG after the first vaccine dose, effective neutralization is delayed.

Together, these findings indicate that CVID-NR fail to mount detectable expansion and differentiation of the S-specific B cell compartment at any time point, whereas CVID-R develop a S-specific B cell response with delayed differentiation kinetics that only later acquire phenotypes and neutralization capacity comparable to HD.

Table 1
Demographic and clinical characteristics of the study cohort

Age - years (median, range)	**Controls (N = 8)**	**CVID-R (N = 7)**	**CVID-NR (N = 5)**	**P-values**
	59.5 (45–73)	**59 (41–67)**	**59 (53–75)**	**0.6904[A]**
Sex (n, %)	5 (62.5%)	4 (57.1)	2 (40%)	0.8541[B]
Female	3 (37.5%)	3 (42.9%)	3 (60%)	
Male				
IGRT (n, %)	0 (0%)	6 (85,7%)	5 (100%)	
Medical history (n, %)	0 (0%)	0 (0%)	5 (100%)	
Autoimmune disorders	1 (12.5%)	0 (0%)	0 (0%)	
Hypertension	0 (0%)	1 (14.3%)	2 (40%)	
Malignancy	0 (0%)	1 (14.3%)	4 (80%)	
Lymphoproliferation	0 (%)	2 (28.5%)	1 (20%)	
Immunosuppressive treatment				
Polysaccharide vaccine response (n, %)	0 (0%)	1 (14.3%)	0 (0%)	
Normal	0 (0%)	4 (57.1%)	3 (60%)	
Poor	8 (100%)	2 (28.5%)	2 (40%)	
Not performed				

[A] Kruskal-Wallis test; [B] Fisher's exact test; IGRT, Immunoglobulin replacement therapy

RSV-F-specific memory reveals defects in long-term B cell maintenance in CVID patients

We next analyzed whether the observed differences in induction of the S-specific B cell response between CVID-R and CVID-NR were also reflected in maintenance of long-lived MBCs by examining the RSV-F-specific B cell compartment. Of note, during the sampling period, RSV infections were uncommon due to lockdown. No differences in RSV-F-specific B cell frequencies and phenotype were observed over time within each group, confirming the stability of a historically encountered antigen (**Figure S3A, B**). Also, no differences in frequencies of RSV^+ B cells were observed between groups (**Figure S3C**). However, clear phenotypic differences of the RSV-F-specific B cell compartment were observed between CVID patients and HD. The frequency of class-switched, IgG^+ and IgA^+, RSV-F-specific B cells was

markedly reduced in CVID patients compared with HD (Fig. 3A, B), in line with previously observed reductions in the MBC compartment [40, 43]. Particularly pronounced reductions were observed in resting IgG^+ and IgA^+ MBC subsets and IgG^+ DN2 (**Figure S3D**). When comparing CVID groups, CVID-R and NR showed largely similar RSV^+ B cell profiles, with the exception of a relative reduction in anergic naïve B cells in CVID-NR when comparing to R (Fig. 3C, D). Together, these findings indicate that CVID patients not only display impaired induction of the B cell response after a (novel) challenge but also defects in the maintenance of long-lived RSV-F-specific MBCs against a historically encountered virus.

CVID patients exhibit a reduced class-switched B cell compartment

Given the marked differential effects observed in class-switched S- and RSV-F-specific B cell responses in CVID patients, we further examined the broader B cell landscape in these individuals to identify potential signatures associated with vaccine responsiveness. 50,000 $CD19^+$ non-S-specific B cells were subsampled from each sample when present (**Figure S4A, B**). This analysis allowed the identification of 13 main B cell populations (Fig. 4A, **Figure S4C, Table S4**). B cell frequencies and phenotypes remained stable across timepoints within the same group (**Figure S4D**). As our aim was to compare the baseline B cell compartment, subsequent analyses were performed at V1pre. The class-switched compartment was markedly impaired in CVID patients compared to HD, affecting both GC-derived and EF populations (Fig. 4B). IgG^+ and IgA^+ MBCs were significantly lower in CVID compared to HD, consistent with previous reports [40, 43, 51, 52]. ASCs, IgA^+ ActBCs, and the EF subsets IgG^+ DN1 and IgA^+ DN2 were also diminished in CVID compared to HD. In contrast, IgD/IgM^+ ActBCs and naïve B cells were relatively more present in CVID patients, a pattern consistent with the pronounced reduction of the class-switched compartment.

To gain further resolution in the class-switched compartment, all IgG^+, IgA^+ and ASC populations within the IgD^- IgM^- $CD19^+$ B cell fraction were subsampled (Fig. 4C, **Figure S4E**). This approach allowed us to better delineate the $CD73^+$ resting MBC compartment and the EF subsets DN1, DN2 and DN3. Interestingly, CVID-R patients, despite their overall reduced frequency, retained a phenotypic distribution comparable to HD, with all main IgG^+ and IgA^+ populations represented (Fig. 4D). In contrast, CVID-NR patients showed an almost complete absence of the switched compartment, with an average of 2% total class-switched B cells compared to 17% observed in HD (Fig. 4E). Most IgG^+ and IgA^+ clusters were either absent or markedly reduced in this group, and only EF-associated IgG^+ subsets, DN1, DN2 and DN3, and IgG^+ MBCs (both $CD73^+$ and $CD73^-$) were detectable, with DN2 representing the most prominent subset in the switched compartment. When comparing CVID-R and NR patients, early MBCs and IgD/IgM^+ $CD21^-$ ActBCs were increased in CVID-NR (**Figure S4F**). The ASC compartment was extremely limited, and the IgA^+ compartment was entirely absent. Overall, these results confirm a profoundly impaired GC-derived response in CVID-NR patients.

IgD/IgM$^-$ CD21$^+$ CD27$^+$ MBCs as an immunological biomarker to predict vaccine responsiveness in CVID patients

Since marked differences between CVID-R and NR were already observed within the class-switched MBC compartment, we examined whether a simplified analysis of the general switched MBC pool before vaccination could distinguish these groups and serve as a correlate of protection to predict vaccine responsiveness. As switched MBCs are routinely assessed in the clinical evaluation of CVID [53], we focused on a gating strategy based on markers already implemented in diagnostic practice, defining switched memory as IgD/IgM$^-$ CD21$^+$ CD27$^+$ B cells within the total CD19$^+$ compartment. By restricting to CD27$^+$ CD21$^+$ cells inclusion of DN subsets was avoided, as these dominate the IgG$^+$ compartment in CVID-NR, potentially confounding group discrimination, and a stable MBC compartment was selected. CVID-NR patients had significantly lower frequencies of IgD/IgM$^-$ CD21$^+$ CD27$^+$ MBCs compared to CVID-R prior to vaccination, and receiver operating characteristic (ROC) analysis identified a cut-off of 0.561% (sensitivity = 100%, 95% confidence interval (CI) = 0.56-1, specificity = 100%, 95% CI = 0.6-1) that separated the two groups with good discriminatory performance, although validation in larger cohorts is needed as the small sample size resulted in wide CI around sensitivity and specificity (Fig. 4E). These findings indicate that switched MBC frequencies within the general B cell compartment may serve as a practical clinical predictor of humoral vaccine responsiveness in CVID.

Discussion

The antigen-specific B cell compartment remains largely unexplored in CVID patients despite its crucial relevance to the heterogenous humoral defects that characterize this disease. Although serological and T cell responses have been examined previously in this population [18, 21, 47, 54], here we provide the first in-depth longitudinal cellular characterization of induction of *de novo* antigen-specific B cell responses to COVID-19 vaccination in patients with CVID. CVID-NR patients showed almost absent S-specific B cells at all timepoints, whereas CVID-R, although delayed in time, developed a S-specific B cell response that is phenotypically comparable to HD 6 months after vaccination. Analysis of the total B cell compartment revealed that CVID-NR consistently exhibit the most severe defects, including an almost complete absence of class-switched populations in contrast to CVID-R that retain a partially preserved class-switched compartment, which was demonstrated to be a predictive parameter for mRNA-based vaccine responsiveness.

COVID-19 vaccination offered a unique opportunity to longitudinally dissect, at high resolution, the B cell characteristics underlying distinct antibody responses in CVID patients after antigen exposure. CVID-NR patients showed a barely detectable S-specific B cell response following vaccination, only present in naïve, IgD/IgM$^+$ B cell populations, in agreement with the absence of detectable antibodies, even after booster vaccination [21]. Interestingly, although EF-associated IgG$^+$ subsets, mainly DN2 B cells, were observed in the general B cell compartment of CVID-NR, this population did not appear within the

S-specific B cell response. This finding is notable since DN2 B cells, which lack CD27 and CD21 expression but express CD11c, have been described to be expanded in autoimmune disorders such as SLE, contributing to the pathogenic response (39,55), in line with the autoimmune background of most CVID-NR patients in the study cohort (Table 1). On the other hand, our previous findings in healthy individuals showed that DN2 B cells are part of the active COVID-19 vaccination responses, arising early and contracting to pre-vaccination levels after six months [22]; a pattern also observed in our HD and CVID-R. Thus, the DN2 B cells observed in the B cell compartment of CVID-NR likely reflect the underlying autoimmune background of these patients rather than indicating a compensatory increase in EF differentiation due to impaired GC activity. Their absence from the S-specific response indicates that EF-associated differentiation does not occur during the induction of a primary immune response, further supporting a broad differentiation impairment affecting both GC- and EF-derived pathways in CVID-NR. Further investigation in a CVID cohort without concomitant autoimmune disease could help disentangle the contribution of autoimmunity to the observed findings.

In line with this, although a relatively increased frequency of IgD/IgM$^+$ CD21^{low} ActBCs was observed in CVID-NR compared with CVID-R in the general B cell compartment; this population was almost absent within the S-specific B cells, which may also be influenced by the limited numbers of cells within this compartment. Previous studies have reported an expansion of CD21^{low} B cells in CVID and associated this phenotype with more complex clinical presentations, underlying immune dysregulation and increased naïve activation (evidenced by increased BCR signaling-related genes) [43, 56, 57]. In this context, the enrichment of IgD/IgM$^+$ CD21^{low} ActBCs in CVID-NR may reflect a state of chronic B cell activation, in line with CD21 downregulation being associated with enhanced negative regulation of BCR signaling [32]. It is therefore tempting to speculate that this might contribute to an increased activation threshold in this population, limiting the capacity of naïve B cells to mount *de novo* responses upon vaccination and potentially explaining the absence of activation and differentiation observed in CVID-NR. However, chronic inflammation and activation alone are unlikely to fully account for the observed group differences. Given the genetic heterogeneity of CVID and the wide range of mutations affecting B cell development and differentiation [41, 43], additional factors may be involved. Although the majority of patients in this study were non-monogenic, variants affecting antigen receptor signaling, B cell activation, GC differentiation, including those in genes such as *PAX5* or *BCL6* or pathways involved in MBC generation [4, 58, 59], may also contribute to differences in responsiveness and require further investigation. Furthermore, T cells play a critical role in immune protection, and underlying T cell defects may contribute to altered B cell composition and clinical manifestations in CVID.

Besides slightly reduced antibody titers and a trend towards reduced frequency of S-specific B cells at V1D28, CVID-R displayed a distinct phenotypic profile at this vaccination time point, with predominantly naïve, unswitched B cells and an almost complete absence of IgG$^+$ and IgA$^+$ MBCs and ActBCs. This impaired cellular response, together with the slight reduction in antibody titers, likely underlies the reduced neutralizing capacity of S-specific antibodies observed at this timepoint. Moreover, the antibody levels detected at V1D28 may originate from a transient, short-lived B cell response that is no longer

detectable at the cellular level at V2D28 or simply in the peripheral compartment. Importantly, although delayed, CVID-R were able to mount a qualitatively normal B cell response after the second vaccine dose, although with reduced IgG^+ MBCs, ultimately achieving S-specific MBC frequencies and phenotypic profiles comparable to HD by V2M6, confirming why sequential vaccinations were beneficial for these CVID patients [21, 60].

To further contextualize antigen-specific induced B cell responses, we examined the RSV-F-specific MBCs compartment as an indicator of long-lived memory maintenance. Both CVID-R and NR exhibited markedly reduced RSV-F-specific resting MBC frequencies compared with HD. These results were not surprising in the case of CVID-NR as they showed a profound impairment of S-specific GC and EF responses. In CVID-R, however, at V2M6, newly formed S-specific MBCs were maintained at levels comparable to HD in addition to a substantial presence of EF DN1 B cells. Altogether, this indicates a proper induction of MBCs upon first antigen exposure, but impaired long-term maintenance of resting MBC populations formed longer ago as evidenced by RSV-F-specific long-lived MBC defects.

Our detailed analysis of the general B cell compartment confirmed previously described abnormalities in CVID, particularly the substantial reduction of the entire class-switched B cell compartment, including ASCs [40, 52, 61–63]. This defect was observed in both CVID-R and CVID-NR but was more pronounced in CVID-NR, in whom class-switched B cells represented around 1% compared to an average of 17% in HD. Furthermore, the switched IgG/IgA^+ MBC compartment, crucial for recall responses, was almost absent. These findings align with the clinical relevance of MBCs in CVID, as their reduced frequency has been associated with absent GC responses, linked to organomegalies, poor prognosis and overall immune dysregulation [40].

Altogether, our findings reveal profound alterations across multiple layers of B cell immunity in CVID, affecting baseline composition, *de novo* induction, and long-lived MBC maintenance. While both CVID-R and CVID-NR exhibit signs of immunological dysfunction, CVID-NR display the most severe defects across all levels of B cell differentiation. Finally, our data demonstrate that analyzing class-switched MBCs, using IgD/IgM^- $CD21^+$ $CD27^+$ as main markers, serves as a distinct immunological signature that distinguishes CVID-R from NR. Although this measurement is already a defined CVID characteristic and validation in larger cohorts is required, the frequency of IgD^- IgM^- $CD21^+$ $CD27^+$ MBCs emerged as a promising predictive parameter for vaccine responsiveness, offering a valuable tool for immunological monitoring in future pandemics. This immunological signature was identified in the unique setting of primary mRNA vaccination during the COVID-19 pandemic, in which vaccine-induced serological responses could be accurately assessed before being influenced by IVIG. This underscores the value of cellular analysis to understand vaccine-induced immunity in this population. Importantly, the measurement of MBCs enables the stratification of patients according to their capacity to mount vaccine-induced humoral immunity, independent of conventional assessments based on polysaccharide vaccine responses. Beyond its potential clinical utility for identifying patients at risk of poor vaccine responsiveness, this signature provides important mechanistic insight into the cellular basis of the heterogeneous serological responses observed in CVID patients. These findings advance our

understanding of vaccine-induced immunity in CVID and establish a framework for the development of more personalized vaccination and immune monitoring strategies in this vulnerable population.

Group members of VACOPID research group

Eric C.M. van Gorp MD PhD, Faye de Wilt BSc, Susanne Bogers MSc, Lennert Gommers BSc, Daryl Geers, Marianne W. van der Ent MSc, P. Martin van Hagen MD PhD, Jelle W. van Haga BSc, Bregtje A. Lemkes MD PhD, Annelou van der Veen BSc, Rogier W. Sanders PhD, Karlijn van der Straten MD, Judith A. Burger BSc, Jacqueline van Rijswijk BSc, Khadija Tejjani BSc, Joey H. Bouhuijs BSc, Karina de Leeuw MD PhD, Annick A.J.M. van de Ven MD PhD, S.F.J. de Kruijf-Bazen MSc, Pieter van Paassen MD PhD, Lotte Wieten PhD, Petra H. Verbeek-Menken BSc, Annelies van Wengen MSc, Anke H.W. Bruns MD PhD, Helen L. Leavis MD PhD, Stefan Nierkens PhD.

Group members of HARMONY research group

The HARMONY research includes the following study groups: VACOPID research group, Target to B research group, Vaccination Against COVID in cancer (VOICE) research group, COVID-19 vaccination response in people with HIV (COVIH) research group, COVID-19 vaccination in immunocompromised patients with hematological malignancies (Cobra-Kai) research group and COVID-19 vaccination in Down Syndrome (PRIDE) research group.

Abbreviations

ActBC
Activated B cell
BAU/ml
Binding antibody units per milliliter
BCR
B cell receptor
CI
Confidence interval
COVID-19
Coronavirus disease-2019
CVID
Common variable immunodeficiency
DN
Double negative
IQR
Interquartile range
IVIG
Intravenous immunoglobulin
MBC

Memory B cell
PBMC
Peripheral Blood Mononuclear Cell
RBD
Receptor binding domain
ROC
Receiver Operating Characteristic
RSV-F
Respiratory Syncytial Virus Fusion protein
S
Spike
SARS-CoV-2
Severe acute respiratory syndrome coronavirus-2

Declarations

Competing Interests

FE reports grants from ZonMw for COVID-19 research (#10430072010007). VASHD received consulting fees from GlaxoSmithKline, Pharming NV for Advisory board meetings and honoraria for lectures from Takeda Pharmaceutical Company, Kedrion, AstraZeneca.

Ethics approval

VACOPID study was conducted in accordance with the Declaration of Helsinki and approved by the Dutch Central Committee on Research Involving Human Subjects (CCMO, NL7647.078.21, EudraCT 2021–000515-24), the Erasmus MC Medical Research Ethics Committee (MEC-2021–0050), and local institutional review boards. Written informed consent was obtained from all participants prior to enrolment.

Funding

This research project was supported by ZonMw (The Netherlands Organization for Health Research and Development) grants #10430072010005 and #10430072010007.

Author Contribution

SMvH, DvB and RDdV led the study. SMvH is the guarantor. SMvH and AtB supervised the study. SMvH, DvB, RDdV, FE conceptualized the study. SMvH, AtB, LFB, RGC, JGV, MvG designed the methodology. LFB, RGC, LB, TJ and RC performed the experiments. LFB, RGC and SMvH verified the overall

replication/reproducibility of the research output. LFB and RGC analyzed and managed the research data. RBC, LFB, SMvH and AtB managed and coordinated the research activity and planning. SMvH, DvB, RDdV, VASHD, FE and JdW acquired the financial support for the project leading to this publication. LFB and RGC visualized the work. LFB, RGC, SMvH and AtB wrote the original draft. All authors reviewed and approved the manuscript.

Acknowledgement

We would like to thank all donors who participated in the HARMONY study, in particular the VACOPID participants, and all the biobank facilities within the Netherlands for processing of samples. We are grateful to Mathieu Claireaux for helping design the methodology and providing the antigen probes and to Sara Garcia-Garcia from the VUmc Core facility for providing technical assistance with the spectral flow cytometry experiments. Furthermore, we would like to thank Corine Geurts van Kessel and Susanne Bogers for obtaining serological data. We would like to acknowledge the funding provided by ZonMw for this study and thank all our HARMONY partners.

Data Availability

All data needed to evaluate the conclusions in the paper are present in the paper and/or the Supplementary Materials.

References

1. Bonilla FA, Barlan I, Chapel H, Costa-Carvalho BT, Cunningham-Rundles C, de la Morena MT, et al. International Consensus Document (ICON): Common Variable Immunodeficiency Disorders. J Allergy Clin Immunol Pract. 2016;4(1):38–59. 07.025 PubMed PMID: 26563668.
2. Ameratunga R, Gillis D, Steele R. Diagnostic criteria for common variable immunodeficiency disorders. J Allergy Clin Immunol Pract. 2016;4(5):1017–8. 10.1016/j.jaip.2016.02.023.
3. Ho HE, Cunningham-Rundles C. Non-infectious Complications of Common Variable Immunodeficiency: Updated Clinical Spectrum, Sequelae, and Insights to Pathogenesis. Front Immunol. 2020;11:149. 10.3389/fimmu.2020.00149 . PubMed PMID: 32117289.
4. IJspeert H, Edwards ESJ, O'Hehir RE, Dalm VASH, van Zelm MC. Update on inborn errors of immunity. J Allergy Clin Immunol. 2025;155(3):740–51. 10.1016/j.jaci.2024. 12.1075 PubMed PMID: 39724969.
5. Azizi G, Abolhassani H, Asgardoon MH, Alinia T, Yazdani R, Mohammadi J, et al. Autoimmunity in common variable immunodeficiency: epidemiology, pathophysiology and management. Expert Rev Clin Immunol. 2017;13(2):101–15. 2016.1224664 PubMed PMID: 27636680.
6. Barbosa RR, Silva SP, Silva SL, Tendeiro R, Melo AC, Pedro E, et al. Monocyte activation is a feature of common variable immunodeficiency irrespective of plasma lipopolysaccharide levels. Clin Exp

Immunol. 2012;169(3):263–72. 10.1111/j.1365-2249.2012.04620. .x PubMed PMID: 22861366.

7. Bateman EAL, Ayers L, Sadler R, Lucas M, Roberts C, Woods A, et al. T cell phenotypes in patients with common variable immunodeficiency disorders: associations with clinical phenotypes in comparison with other groups with recurrent infections. Clin Exp Immunol. 2012;170(2):202–11. 10.1111/j.1365-2249.2012.04643. .x PubMed PMID: 23039891.
8. Cambronero R, Sewell WA, North ME, Webster AD, Farrant J. Up-regulation of IL-12 in monocytes: a fundamental defect in common variable immunodeficiency. J Immunol. 2000;164(1):488–94. 10.4049/jimmunol.164.1.488 . PubMed PMID: 10605046.
9. Edwards ESJ, Bosco JJ, Aui PM, Stirling RG, Cameron PU, Chatelier J et al. Predominantly Antibody-Deficient Patients With Non-infectious Complications Have Reduced Naive B, Treg, Th17, and Tfh17 Cells. Front Immunol. 2019;Volume 10. Available from: https://www.frontiersin.org/journals/immunology/articles/10.3389/fimmu.2019.02593
10. Shields AM, Burns SO, Savic S, Richter AG, Anantharachagan A, Arumugakani G, et al. COVID-19 in patients with primary and secondary immunodeficiency: The United Kingdom experience. J Allergy Clin Immunol. 2021;147(3):870–e8751. 10.1016/j.jaci.2020.12.620.
11. Shields AM, Tadros S, Al-Hakim A, Nell JM, Lin MMN, Chan M, et al. Impact of vaccination on hospitalization and mortality from COVID-19 in patients with primary and secondary immunodeficiency: The United Kingdom experience. Front Immunol. 2022;13:984376. 10.3389/fimmu.2022.984376 . PubMed PMID: 36211396.
12. Ho H en, Mathew S, Peluso MJ, Cunningham-Rundles C. Clinical outcomes and features of COVID-19 in patients with primary immunodeficiencies in New York City. J Allergy Clin Immunol Pract. 2021;9(1):490–e4932. 10.1016/j.jaip.2020.09.052.
13. Giardino G, Milito C, Lougaris V, Punziano A, Carrabba M, Cinetto F, et al. The Impact of SARS-CoV-2 Infection in Patients with Inborn Errors of Immunity: the Experience of the Italian Primary Immunodeficiencies Network (IPINet). J Clin Immunol. 2022;42(5):935–46. 10.1007/s10875-022-01264-y.
14. Meyts I, Bucciol G, Quinti I, Neven B, Fischer A, Seoane E, et al. Coronavirus disease 2019 in patients with inborn errors of immunity: An international study. J Allergy Clin Immunol. 2021;147(2):520–31. 10.1016/j.jaci.2020.09.010.
15. Hartley GE, Edwards ESJ, Bosco JJ, Ojaimi S, Stirling RG, Cameron PU, et al. Influenza-specific IgG1(+) memory B-cell numbers increase upon booster vaccination in healthy adults but not in patients with predominantly antibody deficiency. Clin Transl Immunol. 2020;9(10):e1199. 10.1002/cti2. 1199 PubMed PMID: 33088507.
16. Gardulf A, Abolhassani H, Gustafson R, Eriksson LE, Hammarström L. Predictive markers for humoral influenza vaccine response in patients with common variable immunodeficiency. J Allergy Clin Immunol. 2018;142(6):1922–e19312. 10.1016/j.jaci. 2018.02.052 PubMed PMID: 29678747.
17. Zhan W, Hatchette T, Yue F, Liu J, Song H, Zhao H, et al. Impaired Memory B-Cell Response to Influenza Immunization in Patients With Common Variable Immunodeficiency (CVID). Pathog

Immun. 2021;6(2):105–18. 10.20411/pai.v6i2. 405 PubMed PMID: 34988341.

18. Arroyo-Sánchez D, Cabrera-Marante O, Laguna-Goya R, Almendro-Vázquez P, Carretero O, Gil-Etayo FJ, et al. Immunogenicity of Anti-SARS-CoV-2 Vaccines in Common Variable Immunodeficiency. J Clin Immunol. 2022;42(2):240–52. 10.1007/s10875-021-01174-5 . PubMed PMID: 34787773.
19. Salinas AF, Mortari EP, Terreri S, Quintarelli C, Pulvirenti F, Di Cecca S, et al. SARS-CoV-2 Vaccine Induced Atypical Immune Responses in Antibody Defects: Everybody Does their Best. J Clin Immunol. 2021;41(8):1709–22. 10.1007/s10875-021-01133-0 . PubMed PMID: 34669144.
20. Quinti I, Locatelli F, Carsetti R. The Immune Response to SARS-CoV-2 Vaccination: Insights Learned From Adult Patients With Common Variable Immune Deficiency. Front Immunol. 2022;Volume 12-2021. Available from: https://www.frontiersin.org/journals/immunology/articles/10.3389/fimmu.2021.815404
21. van Leeuwen LPM, Grobben M, GeurtsvanKessel CH, Ellerbroek PM, de Bree GJ, Potjewijd J, et al. Immune Responses 6 Months After mRNA-1273 COVID-19 Vaccination and the Effect of a Third Vaccination in Patients with Inborn Errors of Immunity. J Clin Immunol. 2023;43(6):1104–17. 10.1007/s10875-023-01514-7 . PubMed PMID: 37231290.
22. Fernandez Blanco L, Kuijper LH, Kummer LYL, Verstegen NJM, Bos A, Claireaux M, et al. Heterogeneous Activated B Cell Compartments Arising Early and Transiently After SARS-CoV-2 Vaccination. Eur J Immunol. 2026;56(3):e70165. 10.1002/eji.70165 . PubMed PMID: 41817302.
23. Claireaux M, Elias G, Kerster G, Kuijper LH, Duurland MC, Paul AGA, et al. Deep profiling of B cells responding to various pathogens uncovers compartments in IgG memory B cell and antibody-secreting lineages. Sci Adv. 2025;11(8). 10.1126/sciadv.ado1331.
24. Lopes de Assis F, Hoehn KB, Zhang X, Kardava L, Smith CD, El Merhebi O, et al. Tracking B cell responses to the SARS-CoV-2 mRNA-1273 vaccine. Cell Rep. 2023;42(7):112780. 10.1016/j.celrep.2023.112780.
25. Ciabattini A, Pastore G, Lucchesi S, Montesi G, Costagli S, Polvere J, et al. Trajectory of Spike-Specific B Cells Elicited by Two Doses of BNT162b2 mRNA Vaccine. Cells. 2023;12(13):1706. 10.3390/cells12131706.
26. Sokal A, Chappert P, Barba-Spaeth G, Roeser A, Fourati S, Azzaoui I, et al. Maturation and persistence of the anti-SARS-CoV-2 memory B cell response. Cell. 2021;184(5):1201–e121314. 10.1016/j.cell.2021.01.050.
27. Elsner RA, Shlomchik MJ. Germinal Center and Extrafollicular B Cell Responses in Vaccination, Immunity, and Autoimmunity. Immunity. 2020;53(6):1136–50. 10.1016/j.immuni.2020.11.006.
28. Victora GD, Nussenzweig MC. Annual Review of Immunology Germinal Centers. 2022. 10.1146/annurev-immunol-120419
29. Mesin L, Ersching J, Victora GD, Germinal Center B. Cell Dynamics Immun. 2016;45(3):471–82. 10.1016/j.immuni.2016.09.001.
30. Verstegen NJM, Ubels V, Westerhoff HV, van Ham SM, Barberis M. System-Level Scenarios for the Elucidation of T Cell-Mediated Germinal Center B Cell Differentiation. Front Immunol. 2021;12.

10.3389/fimmu.2021.734282.

31. Tangye SG, Tarlinton DM. Memory B cells: Effectors of long-lived immune responses. Eur J Immunol. 2009;39(8):2065–75. 10.1002/eji.200939531.
32. Lau D, Lan LYL, Andrews SF, Henry C, Rojas KT, Neu KE, et al. Low CD21 expression defines a population of recent germinal center graduates primed for plasma cell differentiation. Sci Immunol. 2017;2(7). 10.1126/sciimmunol.aai8153.
33. Ellebedy AH, Jackson KJL, Kissick HT, Nakaya HI, Davis CW, Roskin KM, et al. Defining antigen-specific plasmablast and memory B cell subsets in human blood after viral infection or vaccination. Nat Immunol. 2016;17(10):1226–34. 10.1038/ni.3533.
34. McGrath JJC, Li L, Wilson PC. Memory B cell diversity: insights for optimized vaccine design. Trends Immunol. 2022;43(5):343–54. 10.1016/j.it.2022.03.005.
35. Steuten J, Bos AV, Kuijper LH, Claireaux M, Olijhoek W, Elias G, et al. Distinct dynamics of antigen-specific induction and differentiation of different CD11c+Tbet + B-cell subsets. J Allergy Clin Immunol. 2023;152(3):689–e6996. 10.1016/j.jaci.2023.02.020.
36. Sachinidis A, Garyfallos A. Double Negative (DN) B cells: A connecting bridge between rheumatic diseases and COVID-19? Mediterr J Rheumatol. 2021;32(3):192. 10.31138/mjr.32.3.192.
37. Perugino CA, Liu H, Feldman J, Marbourg J, Guy TV, Hui A, et al. Two distinct durable human class-switched memory B cell populations are induced by vaccination and infection. Cell Rep. 2025;44(4):115472. 10.1016/. J.CELREP.2025.115472 PubMed PMID: 40173042.
38. Woodruff MC, Ramonell RP, Nguyen DC, Cashman KS, Saini AS, Haddad NS, et al. Extrafollicular B cell responses correlate with neutralizing antibodies and morbidity in COVID-19. Nat Immunol. 2020;21(12):1506–16. 10.1038/s41590-020-00814-z.
39. Gao X, Cockburn IA. The development and function of CD11c+ atypical B cells - insights from single cell analysis. Front Immunol. 2022;13. 10.3389/fimmu.2022.979060.
40. Blanco E, Pérez-Andrés M, Arriba-Méndez S, Serrano C, Criado I, Del Pino-Molina L, et al. Defects in memory B-cell and plasma cell subsets expressing different immunoglobulin-subclasses in patients with CVID and immunoglobulin subclass deficiencies. J Allergy Clin Immunol. 2019;144(3):809–24. https://doi.org/10.1016/j.jaci.2019.02.017.
41. Del Pino Molina L, Torres Canizales JM, Pernía O, Rodríguez Pena R, Ibanez de Caceres I, López Granados E. Defective Bcl-2 expression in memory B cells from common variable immunodeficiency patients. Clin Exp Immunol. 2021;203(3):341–50. 10.1111/cei.13522 . PubMed PMID: 32961586.
42. Rodríguez-Ubreva J, Arutyunyan A, Bonder MJ, Del Pino-Molina L, Clark SJ, de la Calle-Fabregat C, et al. Single-cell Atlas of common variable immunodeficiency shows germinal center-associated epigenetic dysregulation in B-cell responses. Nat Commun. 2022;13(1):1779. 10.1038/s41467-022-29450-x.
43. Rodríguez-Ubreva J, Calafell-Segura J, Calvillo CL, Keller B, Ciudad L, Handfield LF, et al. COVID-19 progression and convalescence in common variable immunodeficiency patients show dysregulated

adaptive immune responses and persistent type I interferon and inflammasome activation. Nat Commun. 2024;15(1):10344. 10.1038/s41467-024-54732-x.

44. Hsieh CL, Goldsmith JA, Schaub JM, DiVenere AM, Kuo HC, Javanmardi K et al. Structure-based design of prefusion-stabilized SARS-CoV-2 spikes. Science (1979). 2020;369(6510):1501–5. 10.1126/science.abd0826
45. Emmaneel A, Quintelier K, Sichien D, Rybakowska P, Marañón C, Alarcón-Riquelme ME, et al. PeacoQC: Peak-based selection of high quality cytometry data. Cytometry Part A. 2022;101(4):325–38. 10.1002/cyto.a.24501.
46. Gassen V, Gaudilliere B, Angst MS, Saeys Y, CytoNorm:. A Normalization Algorithm for Cytometry Data. 2020;(4):268–78. 10.1002/cyto.a.23904
47. van Leeuwen LPM, GeurtsvanKessel CH, Ellerbroek PM, de Bree GJ, Potjewijd J, Rutgers A, et al. Immunogenicity of the mRNA-1273 COVID-19 vaccine in adult patients with inborn errors of immunity. J Allergy Clin Immunol. 2022;149(6):1949–57. 10.1016/j.jaci.2022.04. .002 PubMed PMID: 35421449.
48. GeurtsvanKessel CH, Geers D, Schmitz KS, Mykytyn AZ, Lamers MM, Bogers S, et al. Divergent SARS-CoV-2 Omicron–reactive T and B cell responses in COVID-19 vaccine recipients. Sci Immunol. 2022;7(69). 10.1126/sciimmunol.abo2202.
49. Glass DR, Tsai AG, Oliveria JP, Hartmann FJ, Kimmey SC, Calderon AA, et al. An Integrated Multi-omic Single-Cell Atlas of Human B Cell Identity. Immunity. 2020;53(1):217–e2325. 10.1016/j.immuni.2020.06.013.
50. Kardava L, Rachmaninoff N, Lau WW, Buckner CM, Trihemasava K, Blazkova J et al. Early human B cell signatures of the primary antibody response to mRNA vaccination. Proceedings of the National Academy of Sciences. 2022;119(28). 10.1073/pnas.2204607119
51. Vodjgani M, Aghamohammadi A, Samadi M, Moin M, Hadjati J, Mirahmadian M, et al. Analysis of class-switched memory B cells in patients with common variable immunodeficiency and its clinical implications. J Investig Allergol Clin Immunol. 2007;17(5):321–8. PubMed PMID: 17982925.
52. Haymore BR, Mikita CP, Tsokos GC. Common variable immune deficiency (CVID) presenting as an autoimmune disease: role of memory B cells. Autoimmun Rev. 2008;7(4):309–12. https://doi.org/10.1016/j.autrev.2007.11.024.
53. van Dongen JJM, van der Burg M, Kalina T, Perez-Andres M, Mejstrikova E, Vlkova M, et al. EuroFlow-Based Flowcytometric Diagnostic Screening and Classification of Primary Immunodeficiencies of the Lymphoid System. Front Immunol. 2019;10:1271. 10.3389/fimmu.2019.01271 . PubMed PMID: 31263462.
54. Pulvirenti F, Fernandez Salinas A, Milito C, Terreri S, Piano Mortari E, Quintarelli C, et al. B Cell Response Induced by SARS-CoV-2 Infection Is Boosted by the BNT162b2 Vaccine in Primary Antibody Deficiencies. Cells. 2021;10(11):2915. 10.3390/cells10112915.
55. Jenks SA, Cashman KS, Zumaquero E, Marigorta UM, Patel AV, Wang X, et al. Distinct Effector B Cells Induced by Unregulated Toll-like Receptor 7 Contribute to Pathogenic Responses in Systemic

Lupus Erythematosus. Immunity. 2018;49(4):725–e7396. 10.1016/j.immuni.2018.08.015.

56. Bergman P, Wullimann D, Gao Y, Wahren Borgström E, Norlin AC, Lind Enoksson S, et al. Elevated CD21(low) B Cell Frequency Is a Marker of Poor Immunity to Pfizer-BioNTech BNT162b2 mRNA Vaccine Against SARS-CoV-2 in Patients with Common Variable Immunodeficiency. J Clin Immunol. 2022;42(4):716–27. 10.1007/s10875-022-01244-2 . PubMed PMID: 35290571.
57. Cousin V, Graumann A, Geiger V, Sökler D, Bez P, Gutenberger S, et al. Elevated IL-10 is Linked With the Expansion of T-bethighCD21low B Cells in Patients With Common Variable Immunodeficiency. J Clin Immunol. 2026;46(1):83. 10.1007/s10875-026-02058-2.
58. Kaiser FMP, Gruenbacher S, Oyaga MR, Nio E, Jaritz M, Sun Q, et al. Biallelic PAX5 mutations cause hypogammaglobulinemia, sensorimotor deficits, and autism spectrum disorder. J Exp Med. 2022;219(9):e20220498. 10.1084/jem.20220498.
59. Boast B, Goel S, González-Granado LI, Niemela J, Stoddard J, Edwards ESJ, et al. TCF3 haploinsufficiency defined by immune, clinical, gene-dosage, and murine studies. J Allergy Clin Immunol. 2023;152(3):736–47. 10.1016/j.jaci.2023.05.017.
60. Nielsen BU, Drabe CH, Barnkob MB, Johansen IS, Hansen AKK, Nilsson AC, et al. Antibody response following the third and fourth SARS-CoV-2 vaccine dose in individuals with common variable immunodeficiency. Front Immunol. 2022;13. 10.3389/fimmu.2022.934476.
61. Piqueras B, Lavenu-Bombled C, Galicier L, Cruyssen FBV, Der, Mouthon L, Chevret S, et al. Common Variable Immunodeficiency Patient Classification Based on Impaired B Cell Memory Differentiation Correlates with Clinical Aspects. J Clin Immunol. 2003;23(5):385–400. 10.1023/A:1025373601374.
62. Warnatz K, Denz A, Dräger R, Braun M, Groth C, Wolff-Vorbeck G, et al. Severe deficiency of switched memory B cells (CD27 + IgM – IgD–) in subgroups of patients with common variable immunodeficiency: a new approach to classify a heterogeneous disease. Blood. 2002;99(5):1544–51. 10.1182/blood.V99.5.1544.
63. Wehr C, Kivioja T, Schmitt C, Ferry B, Witte T, Eren E, et al. The EUROclass trial: defining subgroups in common variable immunodeficiency. Blood. 2008;111(1):77–85. 10.1182/blood-2007-06-091744 . PubMed PMID: 17898316.

Figures

Figure 1

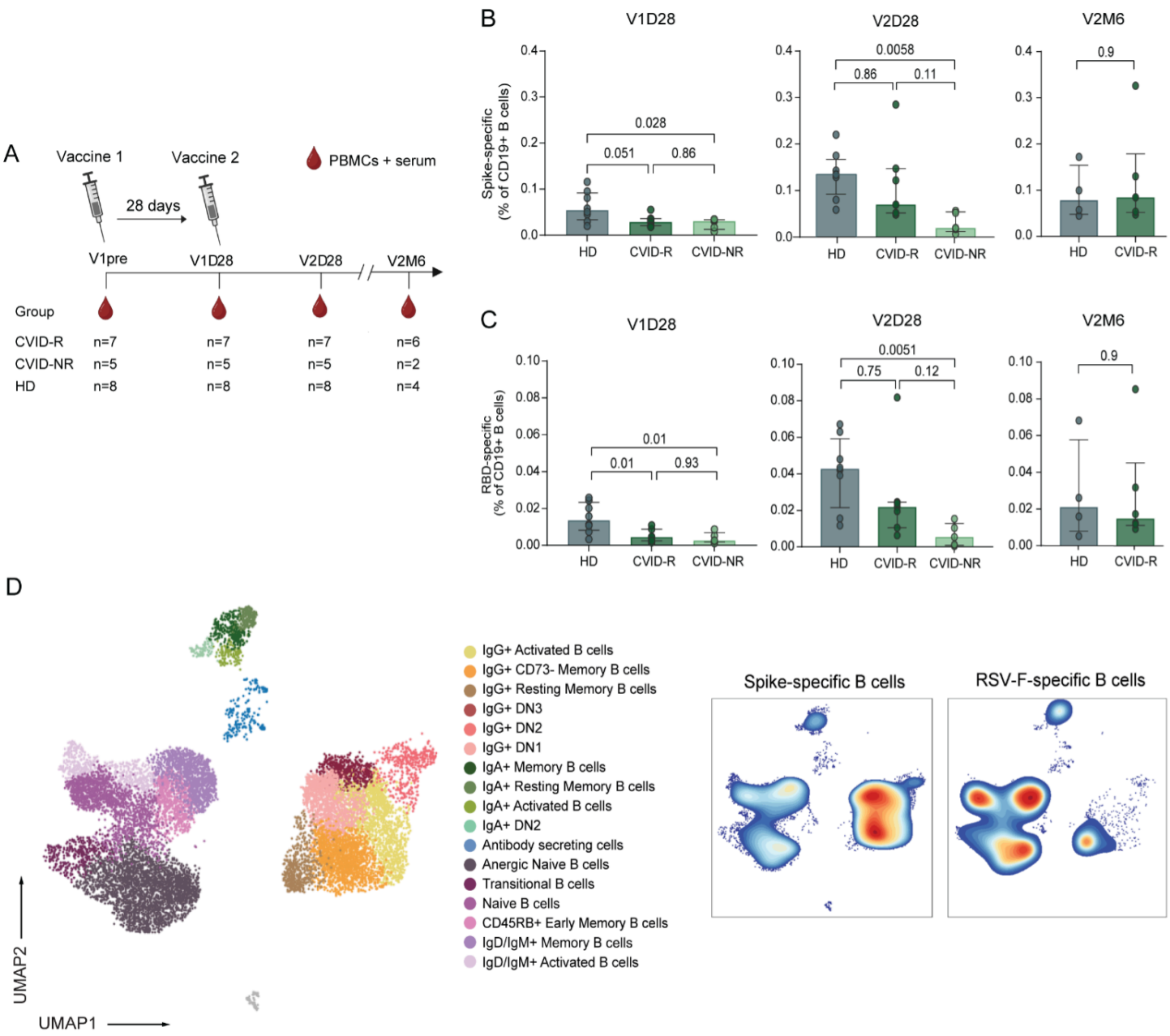


Figure 1

Spike-specific response after SARS-CoV-2 vaccination in CVID patients.

A. Schematic overview of the timeline and study design. PBMCs were collected at baseline (V1pre), 28 days after the first SARS-CoV-2 vaccination (V1D28), 28 days after the second SARS-CoV-2 vaccination (V2D28) and 6 months after the second vaccination (V2M6). **B.** Percentage of S-specific B cells of total $CD19^+$ B cells at V1D28, V2D28 and V2M6. **C.** Percentage of RBD-specific B cells of total $CD19^+$ B cells at V1D28, V2D28 and V2M6. **D.** UMAP projection of all antigen-specific B cells colored by the 17 main populations. All subsequent analysis was focused on the selected 12 CVID patients and 8 HD. S- and

RSV-F-specific B cells overlayed in the UMAP as a density plot. Plotted is the median with interquartile range (IQR) (*P < 0.05, **P < 0.01, ***P < 0.001, ****P < 0.0001).

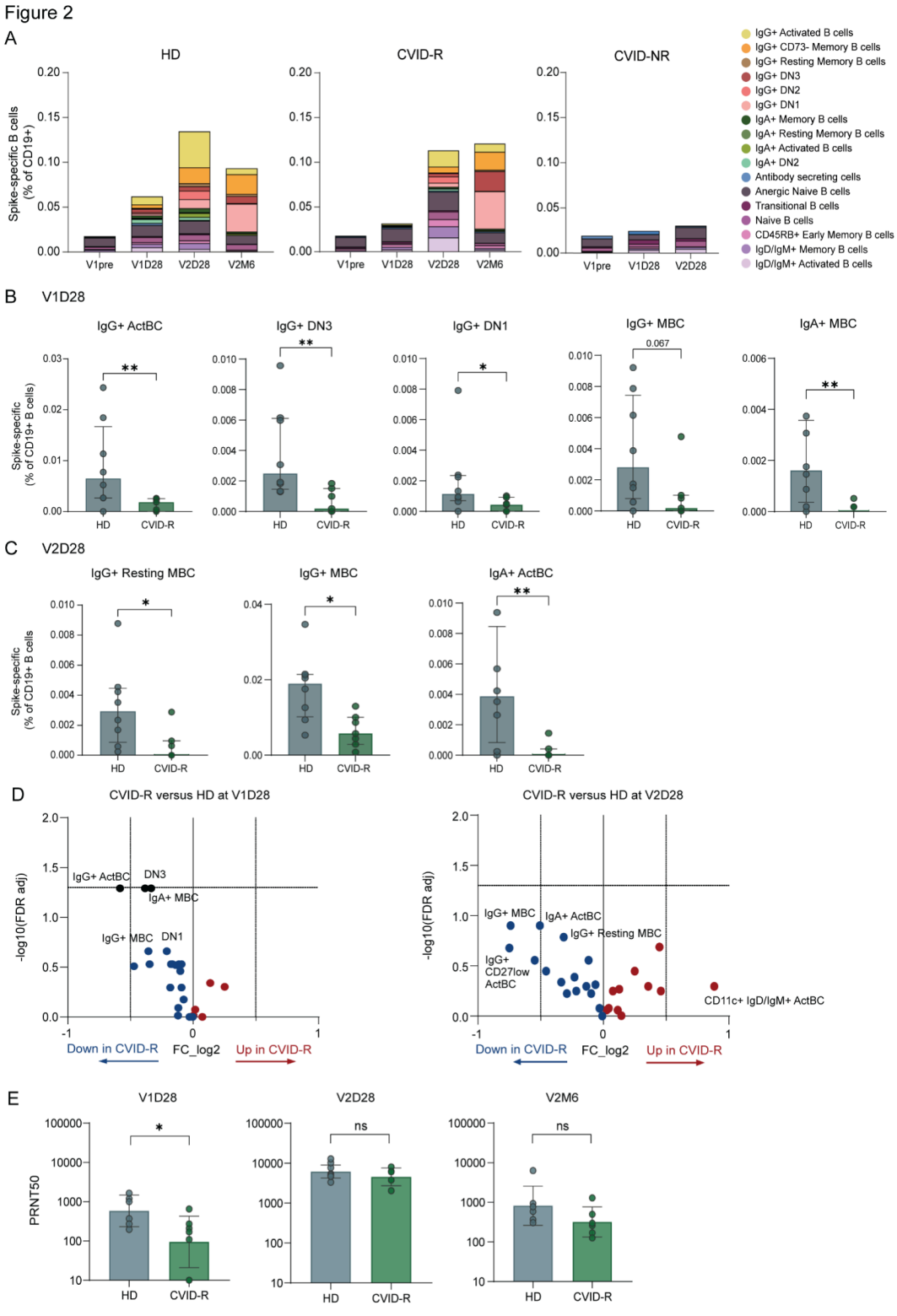


Figure 2

Differential longitudinal dynamics of Spike-specific B cells in CVID.

A. Stacked bar plot showing the mean proportion of S^+ B cells per main population represented as percentage of $CD19^+$ B cells per group. **B.** Percentage of Spike-specific IgG^+ ActBCs, DN1, DN3, MBC and IgA^+ MBCs at V1D28 between HD and CVID-R. **C.** Percentage of Spike-specific IgG^+ resting MBCs, MBCs and IgA^+ ActBCs at V2D28 between HD and CVID-R. **D.** Volcano plot displaying differences in all S^+ B cell clusters frequencies between CVID-R and HD at V1D28 and V2D28. The fold change difference between S^+ B cell clusters is shown on the x-axis, populations with positive FC are higher expressed in CVID-R (red), and with negative FC are higher in HD (blue). The vertical dotted line indicates the threshold set for fold change, at −0.5 and 0.5, respectively. Statistical difference is shown on the y-axis, with a dotted horizontal line indicating a 0.05 p-value. Black dots show statistically different clusters. **E.** Spike-specific neutralization capacity between HD and CVID-R at V1D28 and V2D28. Plaque reduction neutralization test (PRNT). Plotted is the geometric mean with 95% confidence intervals (*P < 0.05, **P < 0.01, ***P < 0.001, ****P < 0.0001).

Figure 3

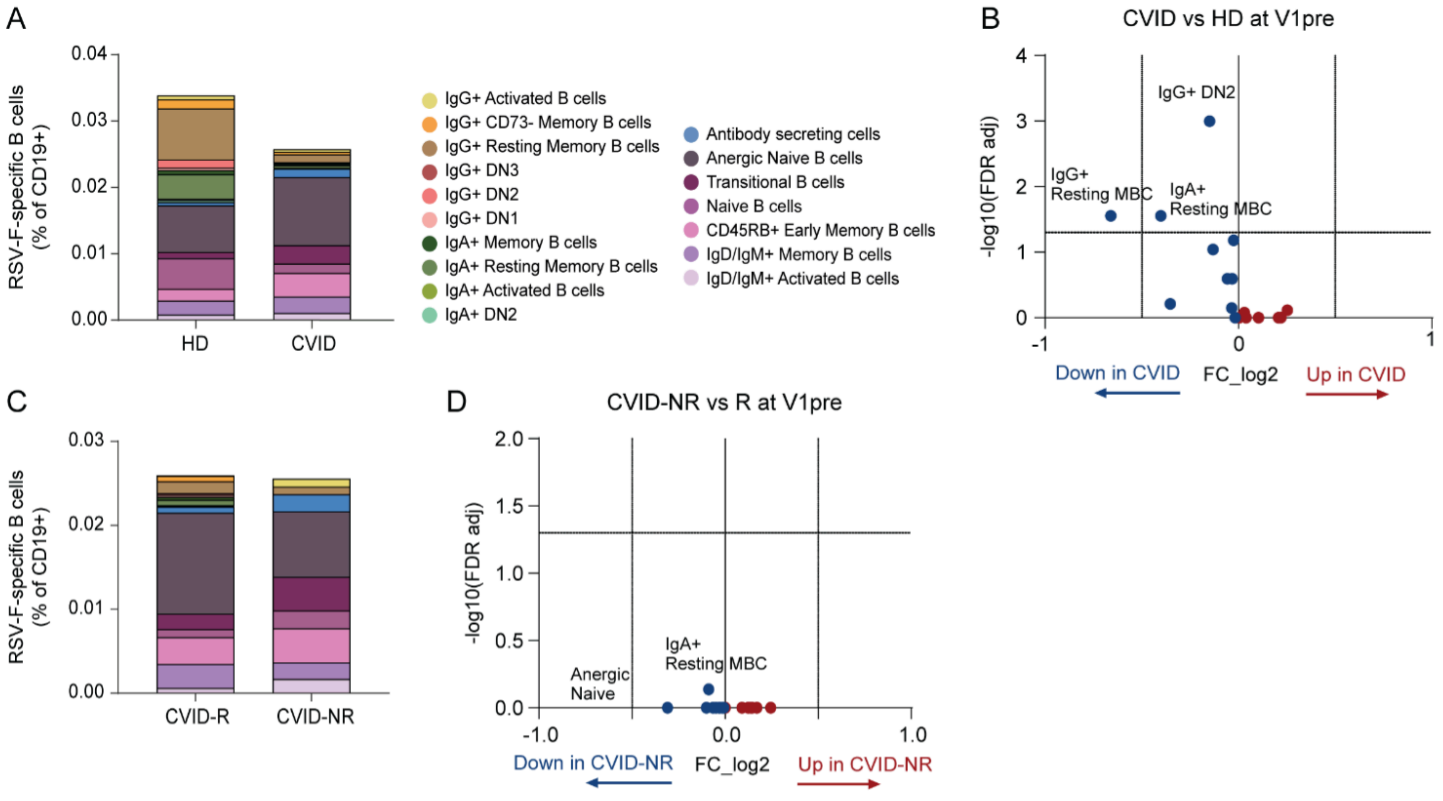


Figure 3

RSV-F-specific resting MBC compartment is impaired in CVID.

A. Stacked bar graph representing the mean proportion of RSV-F^+ B cells (% of $CD19^+$) per main population between HD and total CVID before vaccination (V1pre). **B.** Volcano plot displaying RSV-F^+ B cell populations differentially expressed between CVID and HD at V1pre. The fold change difference between RSV-F^+ B cell populations is shown on the x-axis, populations with positive FC are higher

expressed in CVID (red), and with negative FC are higher in HD (blue). The vertical dotted line indicates the threshold set for fold change, at −0.5 and 0.5, respectively. Statistical difference is shown on the y-axis, with a dotted horizontal line indicating a 0.05 p-value. **C.** Stacked bar plot showing the mean proportion of RSV-F-specific B cells (% of $CD19^{+}$) per main population between CVID-R and CVID-NR at V1pre. **D.** Volcano plot displaying RSV-F^{+} B cell populations differentially expressed between CVID-R and CVID-NR before vaccination. The fold change difference between RSV-F^{+} B cell populations is shown on the x-axis, populations with positive FC are higher expressed in CVID-NR (red), and with negative FC are higher in CVID-R (blue). The vertical dotted line indicates the threshold set for fold change, at −0.5 and 0.5, respectively. Statistical difference is shown on the y-axis, with a dotted horizontal line indicating a 0.05 p-value (*P < 0.05, **P < 0.01, ***P < 0.001, ****P < 0.0001).

Figure 4

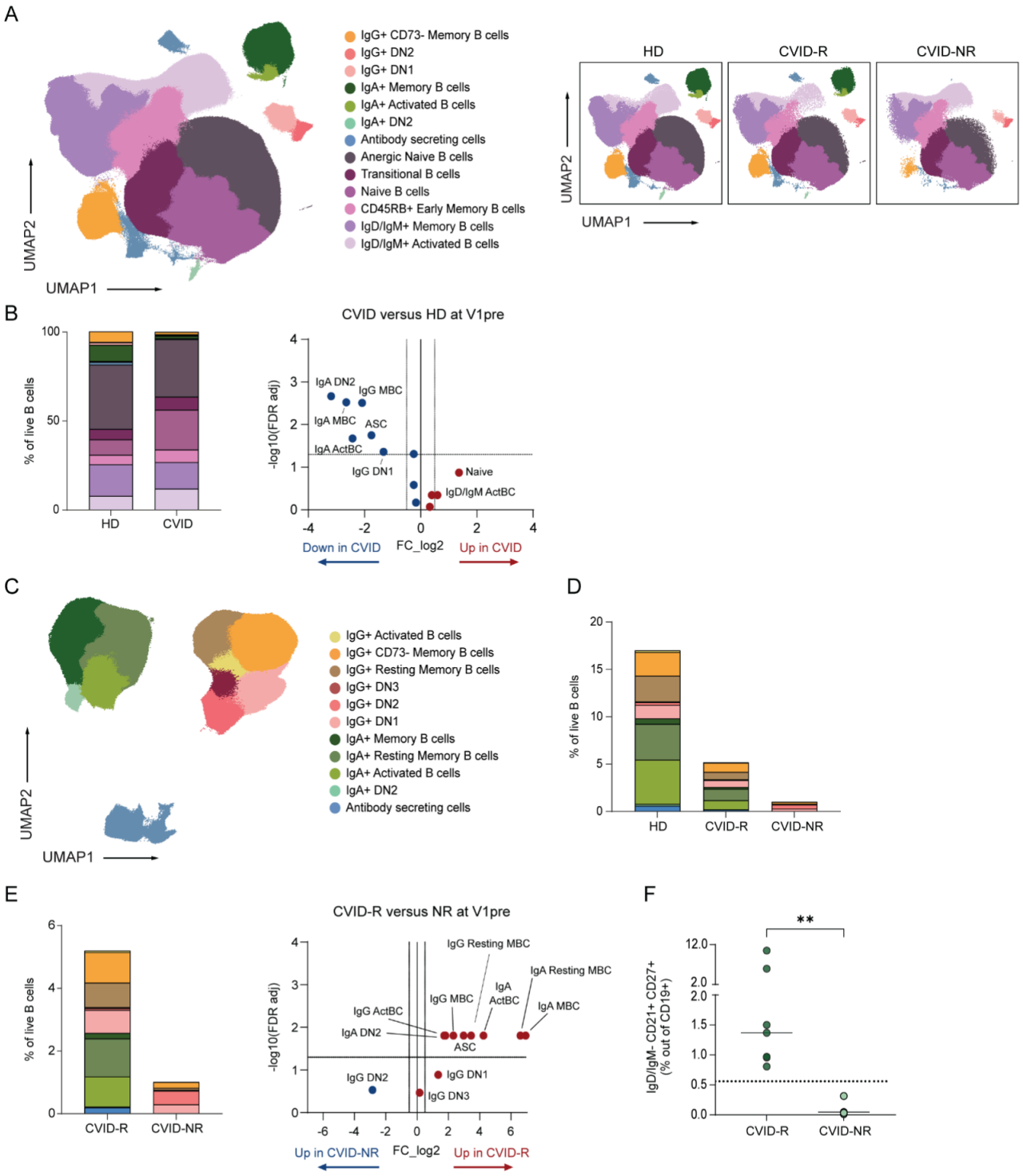


Figure 4

CVID patients showed a reduced class-switched compartment before vaccination.

A. UMAP visualization of CD19^{+} B cells main populations and UMAP projection of B cell populations per group. **B.** Stacked bar graph representing the mean proportion of live CD19^{+} B cells for the 11 main populations between HD and total CVID before vaccination. Volcano plot displaying B cell populations

differentially expressed between CVID and HD at V1pre. The fold change difference between B cell populations is shown on the x-axis, populations with positive FC are higher expressed in CVID (red), and with negative FC are higher in HD (blue). The vertical dotted line indicates the threshold set for fold change, at −0.5 and 0.5, respectively. Statistical difference is shown on the y-axis, with a dotted horizontal line indicating a 0.05 p-value. **C.** UMAP projection of all $CD19^+$ IgG^+ IgA^+ B cells and ASCs. **D.** Stacked bar plot showing the mean proportion of live $CD19^+$ B cells for every population between HD, CVID-R and CVID-NR at V1pre. **E.** Stacked bar plot showing only the differences in B cell populations between CVID-R and CVID-NR at V1pre. Volcano plot displaying class-switched B cell populations differentially expressed between CVID-R and CVID-NR before vaccination. The fold change difference between B cell populations is shown on the x-axis, populations with positive FC are higher expressed in CVID-R (red), and with negative FC are higher in CVID-NR (blue). The vertical dotted line indicates the threshold set for fold change, at −0.5 and 0.5, respectively. Statistical difference is shown on the y-axis, with a dotted horizontal line indicating a 0.05 p-value. **F.** Percentage of IgD/IgM^- $CD21^+$ $CD27^+$ B cells between CVID-R and CVID-NR at V1pre. Dotted horizontal line represents the cutoff of 0.561% determined by ROC analysis that separated the two groups (*P < 0.05, **P < 0.01, ***P < 0.001, ****P < 0.0001).

Supplementary Files

This is a list of supplementary files associated with this preprint. Click to download.

- Supplementalmaterial.pdf
- Supplementarytables.pdf